Hindawi
Advances in Materials Science and Engineering
Volume 2019, Article ID 9896012, 12 pages
https://doi.org/10.1155/2019/9896012

Research Article

Development of Strength for Calcium Aluminate Cement Mortars Blended with GGBS

Hee Jun Yang, Ki Yong Ann, and Min Sun Jung

Department of Civil and Environmental Engineering, Hanyang University, Ansan 15588, Republic of Korea

Correspondence should be addressed to Min Sun Jung; msjcivil@hanyang.ac.kr

Received 5 October 2018; Revised 13 December 2018; Accepted 1 January 2019; Published 13 January 2019

Guest Editor: Joanna Rydz

In the present study, the development of strength in different calcium aluminate cement (CAC) mixture mortars with granulated ground blast-furnace slag (GGBS) was investigated. The substitution of GGBS levels was 0, 20, 40, and 60% weight of binder, of which the CAC used in this study naturally contained C_2AS clinker as a secondary phase. To activate a hydraulic nature of the phase, in addition to the mineral additive, all specimens were cured at $35 \pm 2^{\circ}C$ for the first 24 hours and then stored in a 95% humidity chamber at $25 \pm 2^{\circ}C$. The penetration resistance of fresh mortar was measured immediately after pouring, and the mortar compressive strength was monitored for 365 days. Simultaneously, to evaluate the hydration kinetics at early ages, in terms of heat evolution, the calorimetric analysis was performed at the isothermal condition ($35^{\circ}C$) for 24 hours. The hydration behavior in the long term was characterized by X-ray diffraction, which was supported by microscopic observation using scanning electron microscopy with energy dispersive spectroscopy. Furthermore, an examination of the pore structure was accompanied to quantify the porosity. As a result, it was found that an increase in the GGBS content in the mixture resulted in an increased setting time, as well as total heat evolved for 24 hours in normalized calorimetry curves. In addition, the strength development of mortar showed a continuous increased value up to 365 days, accounting 43.8–57.5 MPa for the mixtures, due to a formation of stratlingite, which was identified at the pastes cured for 365 days using chemical and microscopic analysis. However, GGBS replacement did not affect on the pore size distribution in the cement matrix, except for total intrusion volume.

1. Introduction

Calcium aluminate cement (CAC), mainly consisting of monocalcium aluminate (CA), has been used in the construction industry since the late 19th and early 20th centuries after patented in 1908 by J. Bied [1–3]. Although it was initially developed to enhance the resistance to aggrieve ions (sulfates and chlorides), as an alternative to Portland cement, a rapid strength development at early ages (within 24 hours) led to its application to military facilities in World War I, resulting in production of the various of types of CAC [1–3]. Nowadays, the use of CAC in specific fields is involved in a wide range, including as a fire-resistant material in refractory application [4–6], a high resistance against chemical degradations in the industrial floor and wastewater application [7–9], rapid setting and hardening grout in tunnel lining [1], and resistance to abrasion in hydraulic dam spillway [7]. In addition, ability in gaining the strength rapidly, even at lower temperatures below $0^{\circ}C$, makes it possible to cold weather concreting [10]. Recently, there is an increasing interest in the use of CAC with expansive agents as a repair material [11, 12].

Despite high performance, a structural use of CAC in construction has been faced with a critical problem, a loss of strength due to the conversion process; metastable hydration products (CAH_{10} and C_2AH_8) are thermodynamically transformed into stable ones (C_3AH_6 and AH_3), depending on curing regimes and ages, as follows [1,10,13–16]:

$$3CAH_{10} \longrightarrow C_3AH_6 + 2AH_3 + 18H \quad (1)$$

$$3C_2AH_{10} \longrightarrow 2C_3AH_6 + AH_3 + 9H \quad (2)$$

The cubic phases of C_3AH_6 and AH_3 have the higher density in CAC hydration; therefore, the space filled by low-density hexagonal phases of CAH_{10} and C_2AH_8, which

produces a high early strength, would be decreased after the conversion process, resulting in a sudden reduction in the strength [1, 13]. Many previous studies [17–20] reported that long-term properties of CAC concrete exhibited a decreased strength, compared to the strength at early ages. It has been attempted to take some precautions for avoiding/eliminating the transformation of metastable hydrates using chemical and mineral admixtures, to overcome this anxiety about instability to the properties over time. Falzone et al. [21] recently investigated the conversion bypassing effect of calcium nitrate added in CAC paste, on the basis of the thermodynamic selectivity mechanism, but most of the studies have focused on the substitution of siliceous materials in the CAC-based binder system [22–31].

Midgley and Rao [22] raised an influence of strätlingite on mechanical properties of high alumina cement (HAC) and suggested that the possible formation of C_2ASH_8 hydrate would compensate a reduced compressive strength after conversion at the normal temperature (20°C). It was confirmed by Majumdar and coworkers [23, 24] that the formation of C_2ASH_8 hydrate improved the strength development for two types of commercial CAC (Ciment Fondu and Secar 71), replaced by GGBS in 50% weight of binder, at 20 and 40°C. Moreover, the authors investigated the properties of CAC with various pozzolanic materials, such as natural pozzolan and metakaolin, and concluded that substitution of siliceous materials in CAC enhanced the strength development and sulfate resistance depending on types of binder and their replacement ratio, which could impose the different levels of silica in the solution [25]. The ability of silicate ions in generating the strätlingite in the CAC-based binary system, consisting of fly ash or silica fume, was also reported in the previous studies [26–30]. In addition, Gosselin et al. [28] carried out the observation of microstructural development of CAC, containing C_2AS clinker as the secondary phase, and demonstrated that higher curing temperatures (above 38°C) for the first 24 hours imposed the formation of C_2ASH_8 hydrates, even at early ages, which in turn resulted in the densification of the matrix.

However, most of the studies [22–25] focused on the transformation of the metastable hydrates into C_2ASH_8 in the presence of reactive silicates using Ciment Fondu, consisting of the CA clinker as a main hydraulic phase. Otherwise, only hydration behavior was revealed using cement paste made with CAC containing the C_2AS clinker, which could produce the strätlingite directly [26–30]. In this study, therefore, to evaluate the influence of GGBS replacement on mechanical properties in the mortar of CAC-GGBS mixtures, the development of strength was investigated by setting time and compressive strength. The strength for mortars of CAC-GGBS mixtures cured at a given regime was monitored for 365 days. Simultaneously, isothermal calorimetry and X-ray diffraction analysis were performed to identify the hydration behavior, particularly for a formation of strätlingite and its influence on mitigation in the conversion reaction, at early and long-term age, of which the morphology of the phase was inspected by scanning electron microscopy. Furthermore, the pore distribution was examined by the volume of mercury intruded into a specimen to verify a modification of the pore structure, arising from the substitution of GGBS in CAC. The CAC containing 52.0% of Al_2O_3 content in the cement was used, of which the C_2AS phase naturally occurred.

2. Experimental Works

To evaluate the influence of a formation of calcium aluminates hydrate containing silicates (i.e., strätlingite, C_2ASH_8) in the hydration process on the fundamental properties for CAC mortar, three levels of replacement in GGBS (20, 40, and 60% by weight of cement) were used in this study. The oxide composition of the binders determined by X-ray fluorescence (XRF) and mix proportions for the specimens are given in Tables 1 and 2, respectively, and also XRD curves of the materials are shown in Figure 1. All specimens for the experiments were manufactured without any admixtures to avoid the influence of the chemical effect on the CAC matrix and were kept at 0.4 of a total W/C. Based on the facts that CAC could achieve 80 percent of ultimate strength within 24 hours due to rapid hydration [1–3] and accelerate the formation of the C_2ASH_8 hydrate in the pozzolan blends system at above 30°C of the curing temperature [32], the specimens were cured in a humidity chamber (RH 95%) at 35 ± 2°C for 24 hours and after that was stored in the chamber at 25 ± 2°C to simulate the moderate situation for 364 days. As the elevated temperatures during evaporation of a free water from pores in the matrix (i.e., hydration stopping method) could encourage the transformation of hexagonal phases into cubic ones, the samples were immersed in isopropanol for 7 days in a low-temperature chamber (below 0°C), which was subsequently placed in a vacuum desiccator to remove the residual solvent and/or water from the sample before measurement.

2.1. Measurement of Heat Evolution. Isothermal calorimetry is a useful technique to study the kinetics of the hydration process, of which the heat flow is directly measured and monitored for a specified duration under controlled conditions. Approximately 10 g of the premixed dry powder at the given proportions (Table 2) was placed in an admix glass ampoule and set up within the calorimeter. Then, a distilled water equivalent to 0.4 of total water to binder ratio was injected from the syringe system and continuously stirred during test duration. The rate of heat evolution at the isothermal condition (35°C) was measured and recorded for 24 hours using a TAM air 3-channel calorimeter and thermostat (TA Instruments). Total heat evolution of the sample was calculated by integration of the rate curve for a given time. After obtaining the calorimetric results, it was normalized by mass of CAC content to determine an influence of CAC solely on the rate of heat evolution and its cumulative one at a given W/B.

2.2. Testing of Strength. A fresh mortar with a proportion of 1.00 : 0.40 : 2.45 for the cement : water : sand was mixed and then placed in a prism mold ($100 \times 100 \times 400$ mm) to

Table 1: Chemical composition of binders used in this study.

Oxides (%)	CAC	GGBS
CaO	38.83	47.18
Al_2O_3	52.03	13.13
SiO_2	5.02	29.70
Fe_2O_3	0.86	0.64
SO_3	0.09	2.30
MgO	0.42	4.55
K_2O	0.68	0.53
Na_2O	0.17	0.22
MnO	0.03	0.29
Ignition loss	0.53	1.29
Fineness (cm^2/g)	5,150	5,420
Density (g/cm^3)	3.03	2.93

Table 2: Mix proportions for experimental works.

	Abbreviation	Weight ratio				Experiments
		CAC	GGBS	Water	Sand	
Paste	CAC 100	1.00	0.00	0.4	—	Calorimetry XRD SEM/EDS
	CAC 80	0.80	0.20			
	CAC 60	0.60	0.40			
	CAC 40	0.40	0.60			
Mortar	CAC 100	1.00	0.00	0.4	2.45	Setting time Compressive strength MIP
	CAC 80	0.80	0.20			
	CAC 60	0.60	0.40			
	CAC 40	0.40	0.60			

determine the penetration resistance with time, which was subsequently measured using a series of standard needles (Ø4.52, 6.4, 9.1, 14.3, 20.2, and 28.6 mm) at various time intervals [33]. The test was performed in a room chamber at $35 \pm 2^{\circ}$C, RH 95%. After obtaining the relation between penetration resistance and time, which was fitted by a suitable function (usually, exponential one), the setting time was determined by assuming that the initial and final sets were defined as time taken to reach at 3.4 and 27.5 MPa against penetration resistance, respectively.

To monitor development of compressive strength, mortar specimens were fabricated in a cubic mold ($50 \times 50 \times 50$ mm) with the equal mix proportion to the penetration resistance test. After casting, the mortar specimens were precured in the 95% RH humidity chamber at $35 \pm 2^{\circ}$C for 24 hours and then demolded. In turn, the specimens were stored in the chamber at $25 \pm 2^{\circ}$C for 364 days. The compressive strength for mortar specimens was measured at various ages (1, 7, 28, 98, 180, and 365 days). The replication of each mix for the compressive strength of mortar was six, and their average value was taken in plotting the variation at a given age.

2.3. Identification of Hydration Products. To observe the formation of hydration products with time, the paste specimens were fabricated into a thin mold ($10 \times 50 \times 50$ mm), which would impose less potential to transform metastable hydrates (CAH_{10} and C_2AH_8) into stable ones (C_3AH_6 and AH_3) arising from self-heating at early hydration. All pastes were kept at 0.4 of W/B. After curing for 1, 98, and 365 days through the identical procedure to the mortar specimen for compressive strength, the specimens adapted the hydration stopping method and then crushed/ground to obtain the dust sample, which in turn was sieved with a 75 μm sieve. Then, the powder sample was stored in a vacuum desiccator to avoid the carbonation reaction before measurement. The XRD test was carried out with the D/MAX-2500 diffractometer (Rigaku Corp.) using Cu Kα1 radiation with a wavelength of 1.54 Å. The scan range was from 5 to 45° of 2θ at a scan rate of 4°min. The presence of hydration products in the XRD curve was confirmed using Jade 9.5 software with PDF-2 database from International Center for Diffraction Data (ICDD).

2.4. Examination of Pore Structure. To check an influence of GGBS replacement on the pore structure of the matrix in the blends system at a given age, mercury intrusion porosimetry (MIP) was performed using the identical mortar specimens for compressive strength. After 365 days of curing, the mortars were crushed into a piece of about 1 cm^3, followed by removal of the residual water using the alcohol-based solvent under low temperature. Then, the specimens were stored in a vacuum desiccator to remove/evaporate the free water totally, before testing. The equipment used in this study was Autopore IV 9500 (Micromeritics Instrument Corp.) with two devices, of which a low pressure of mercury was applied up to 0.2 MPa using nitrogen gas to measure large porosity, and then the pressure was progressively increased to 227.5 MPa for a small one. A contact angle and a surface tension of mercury were assumed 130° and 485×10^{-3} N/m, respectively. The pore diameter, which was calculated by the Washburn equation at a given pressure (Equation (3)), was plotted in the cumulative and log differential intrusion curve, respectively:

$$d = \frac{-4\gamma \cos\theta}{P}, \tag{3}$$

where d is the pore diameter (m), γ is the surface tension of mercury (N/m), θ is the contact angle of the mercury with the sample (°), and P is the applied pressure (MPa).

2.5. Microscopic Observation of Morphology. Scanning electron microscopic (SEM) analysis is widely used for the inspection of the morphology of phases, and simultaneously, the elemental examination for the phases can be possible using the energy dispersive spectroscopy (EDS) method. The paste of CAC-GGBS mixtures, identical to the XRD test, was crushed into a piece of 1-2 cm^2, which subsequently was immersed in an isopropanol solvent for 7 days in a cooling chamber at below 0°C. This procedure was able to remove the free water within the specimen, preserving the hydration products unchanged during hydration stopping treatment. After stored in a vacuum desiccator to evaporate the residual water/solvent on the surface for 2 days, the sample was placed/fixed into the metallic plate and coated in platinum. The microscopic observations were performed by FE-SEM using S-4800 (Hitachi) with instrumental parameters, which were an accelerating voltage of 15 kV, the working distance

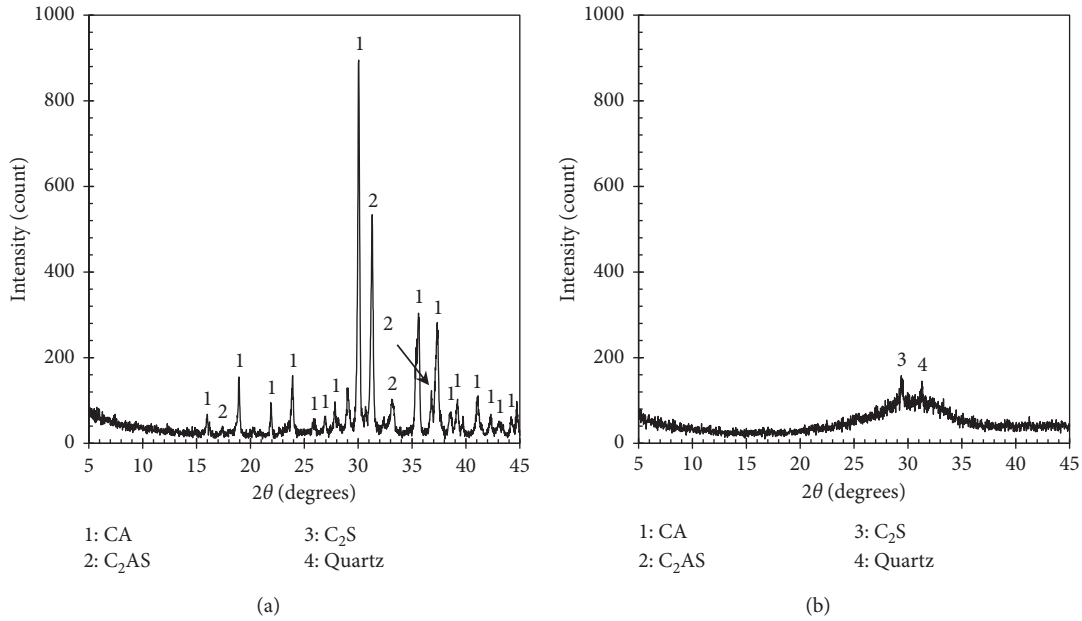

Figure 1: XRD curves of raw materials used in this study: (a) CAC; (b) GGBS.

of 11–13 mm, and magnification of ×10,000, in conjunction with the EDS analyzer for chemical analysis. The measurements at each sample were carried out 30 times, and each spectrum was collected until exposure time reached 1,000 counts in the intensity.

3. Results and Discussion

3.1. Evolution of Hydration Heat. The heat flow and its cumulative curves for the mixtures of CAC and GGBS at 35°C of the isothermal condition for 24 hours, of which the cement was partially substituted by GGBS (0, 20, 40, and 60%), are shown in Figure 2. It is evident that replacement of GGBS was crucial for all CAC-GGBS blends in the kinetics of hydration; an increase of GGBS content in the binder system resulted in a decrease in the total amount of heat released for 24 hours. For example, CAC 100 ranked the highest value of 334.1 J/g in cumulative heat evolution for 24 hours, while CAC 80, 60, and 40 indicated 283.6, 252.9, and 179.1 J/g, respectively. However, the first peak for the rate of heat evolution, during which concentration of Ca^{2+} and $Al(OH)_4^-$ ions would be achieved a maximum level in the solution [10], showed a marginal difference between CAC-GGBS mixtures. In fact, early hydration of CAC may be affected by the insufficiency of available water, space, and reactant. Gosselin et al. [28] investigated the hydration behavior of CAC at isothermal temperatures of 20, 38, and 70°C using calorimetry and XRD analysis and revealed that the primary reactive phase (i.e., CA) still existed after reaching the main peak in the calorimetry curve, except for the case of 70°C. From the experiment works by Ideker [34], moreover, it was found that chemical shrinkage of CAC (mentioned as GCX) showed a convergent trend under isothermal conditions (20 and 38°C), before which the variation of water in the plastic vial approached to a maximum level relevant to the massive precipitation of hydrates. These results mean that a surplus of water in the matrix would be available after the initial hydration process. Based on these observations, it may be assumed that CAC hydration at the initial periods is dominated by available space in the matrix and, furthermore, conjectured that replacement of GGBS with CAC allows further hydration at a given age. This hypothesis was supported by previous studies [29, 32] that the CAC blends system replaced by lower density binder exhibited more exothermic reaction, compared to the CAC alone. This phenomenon ensured that the calorimetry curve in the present work was normalized to CAC content, as shown in Figure 3. The transformed curves for heat flow showed a dependency of GGBS replacement on the initial reaction of CAC-GGBS mixture, of which the increase of the GGBS content in the system resulted in an increase in the rate of heat evolution within 2 hours. In addition, the cumulative heat curve was increased with the increase in substitution of GGBS in the mixture, of which CAC 40 produced the highest value of 447.8 J/g for the total heat released for 24 hours.

3.2. Phase Composition. The hydration products for the paste of CAC-GGBS mixtures at a given curing regime were investigated by the X-ray diffraction method with curing ages, as shown in Figure 4. An identification of the phases was carried out based on crystallographic data from ICDD. The XRD curves in CAC paste were affected by the presence of GGBS in the mixture. The hexagonal phase of C_2AH_8 was dominantly formed at 1 day, regardless of mixture types, but C_3AH_6 and AH_3 were detected at only the case of CAC 100. In the long-term hydration, it was clearly shown that the transformation of C_2AH_8 into cubic phases (i.e., C_3AH_6 and AH_3) is restricted by the substitution of GGBS in CAC. At 28 days of curing, CAC 100 showed a large increase in the peak intensity for C_3AH_6 and AH_3 hydrates, resulting in a

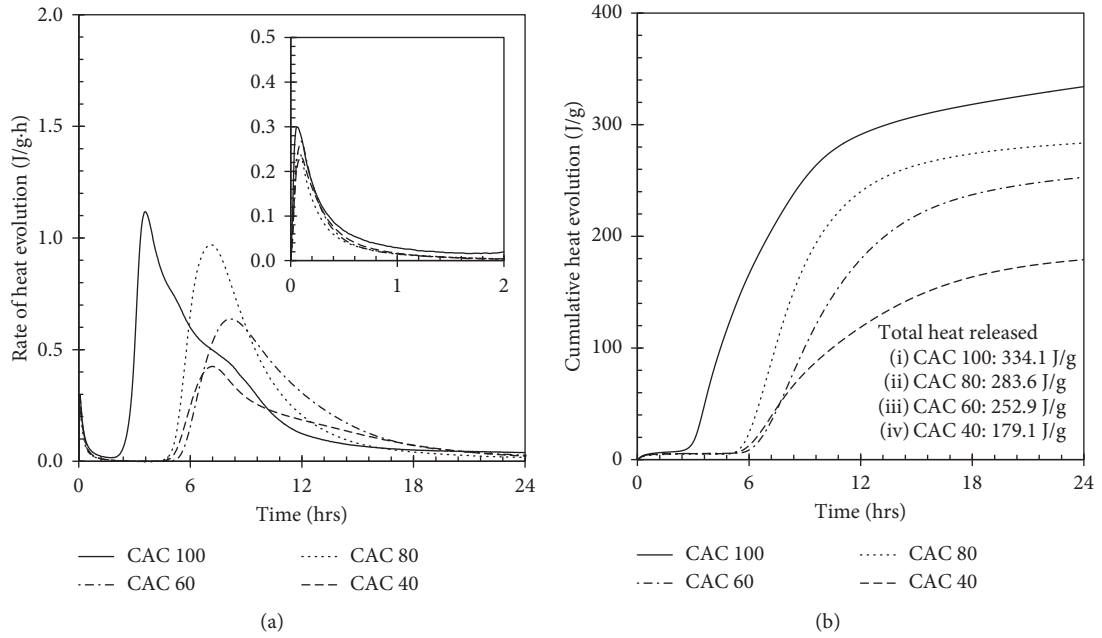

Figure 2: Calorimetric curves for CAC-GGBS mixtures with 0.4 of W/B ratio at an isothermal of 35°C for 24 hours: (a) rate of heat evolution; (b) cumulative heat evolution.

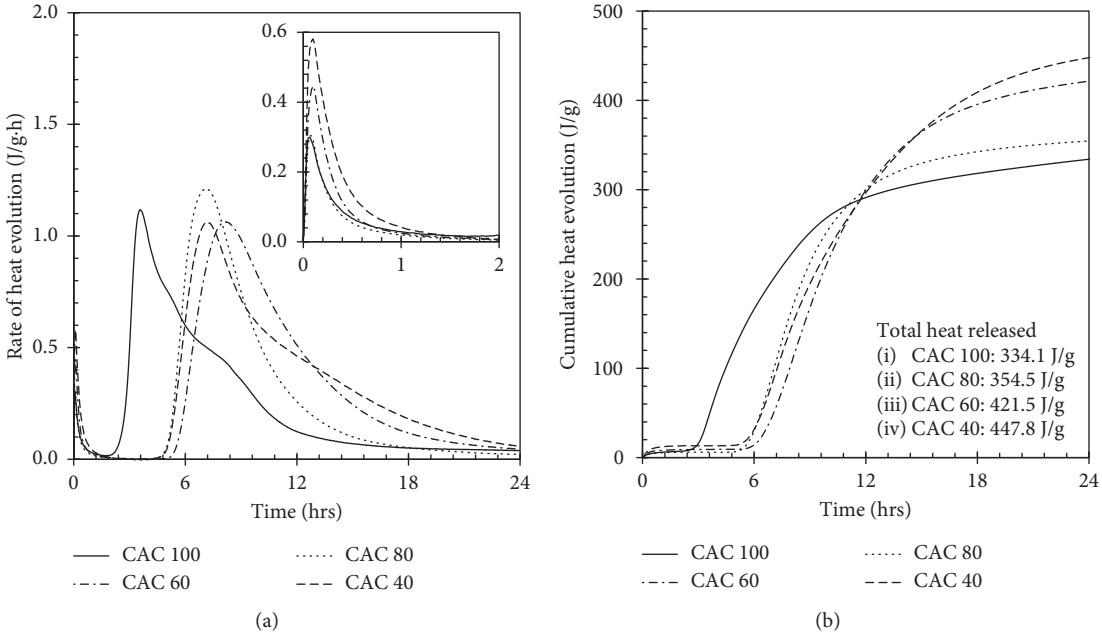

Figure 3: Calorimetric curves normalized to CAC content: (a) rate of heat evolution; (b) cumulative heat evolution.

disappearance of C_2AH_8, which means the metastable hydrates fully converted. In contrast, the binary system of CAC and GGBS indicated a vanished C_2AH_8 hydrate but simultaneously a formation of C_2ASH_8 hydrate, depending on GGBS content in the CAC. In fact, CAC containing higher SiO_2 content (4-5%) naturally possesses the amount of the C_2AS phase, which has low hydraulic properties at normal temperatures (below 20°C) [29]. However, it was observed by Gosselin [32] that hydration of C_2AS in the assemblage C_2AH_8 and C_3AH_6 (i.e., specimens cured at 38 and 70°C) resulted in the precipitation of C_2ASH_8 hydrate, even at early ages. Moreover, in the presence of pozzolanic materials (GGBS, PFA, and SF) in the CAC mixture, the formation of C_2ASH_8 hydrate can be accelerated due to a release of reactive silica into the solution, which in turn reacted with calcium aluminates hydrates in accordance to following equations [27]:

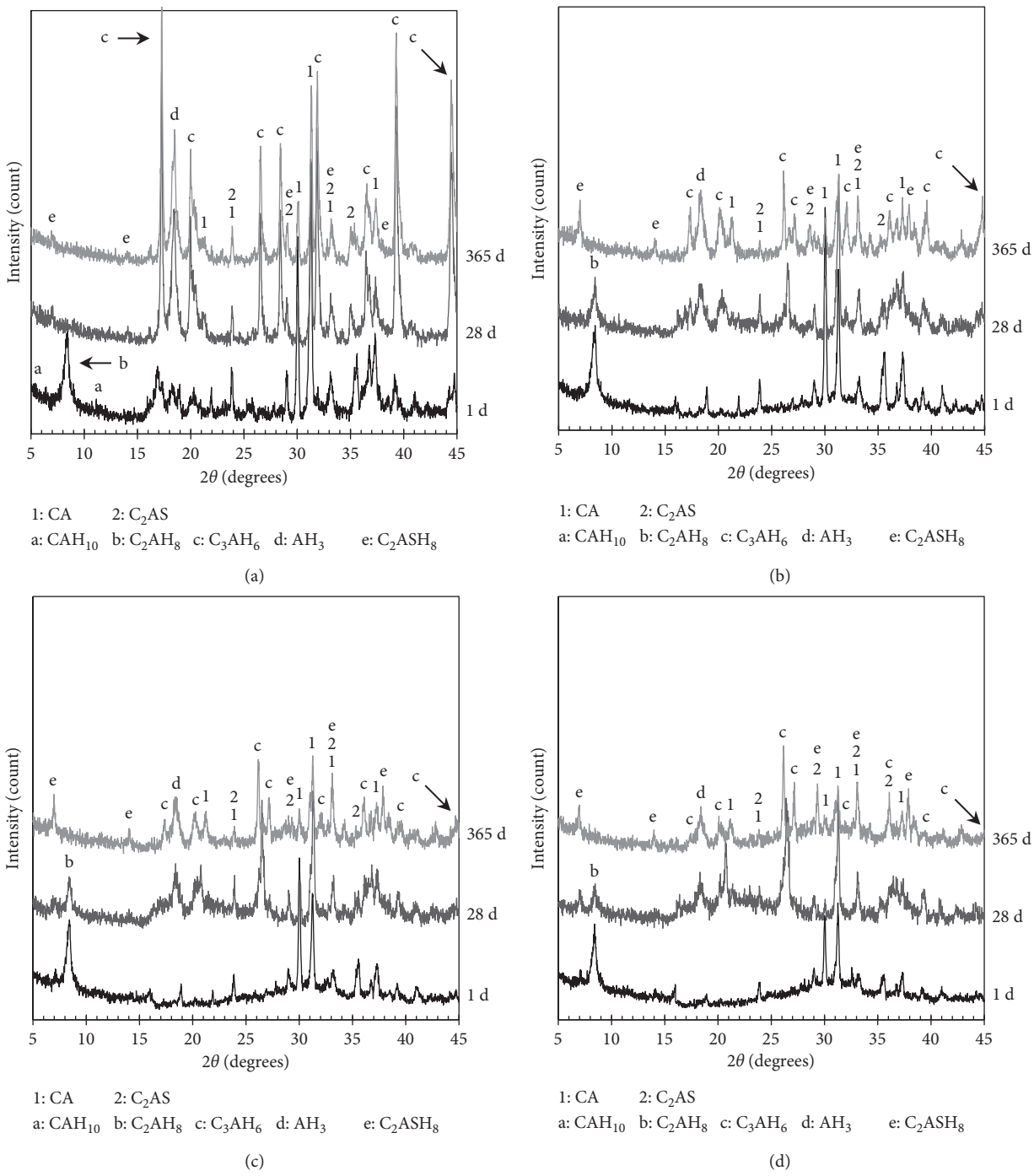

Figure 4: XRD curves for paste of CAC-GGBS mixtures at 0.4 of W/B with time: (a) CAC 100; (b) CAC 80; (c) CAC 60; (d) CAC 40.

$$2CAH_{10} \xrightarrow{S} C_2ASH_8 + AH_3 + 9H \quad (4)$$

$$C_2AH_8 \xrightarrow{S} C_2ASH_8 \quad (5)$$

This reaction could be controlled by the amounts of silicate ions in the solution (i.e., dissolution behavior of the siliceous materials). As an increased GGBS content is more probable of producing the silicate ions in the hydration process, the formation of C_2ASH_8 hydrate would be promoted at a given condition. However, the increased GGBS content would accompany a decrease in the content of hydraulic phases in the binder system, and simultaneously, the large amounts of unreacted GGBS in the matrix may prevent further hydration in the long-term hydration, blocking the CAC particles to contact with water, thereby resulting in a low strength of CAC. This phenomenon will be discussed in the next section.

3.3. Development of Strength. The curves for the resistance against penetration of fresh CAC-GGBS blended mortars with time are given in Figure 5, of which the initial and final

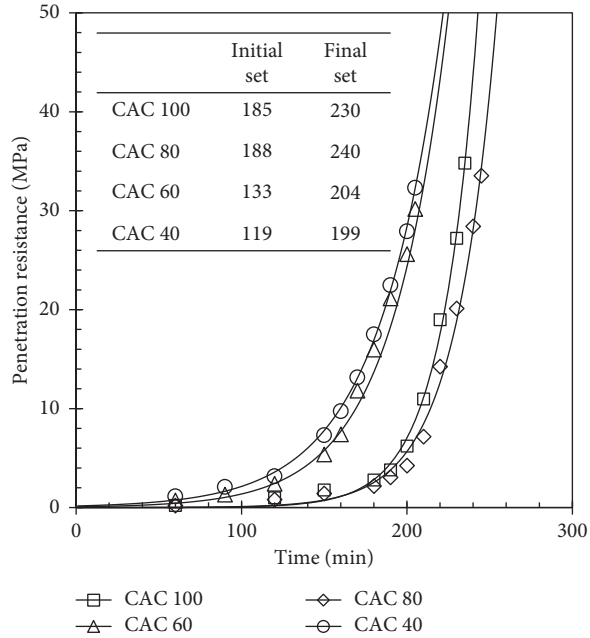

Figure 5: Penetration resistance with time for fresh mortar of CAC-GGBS mixtures. The curve is fitted by an exponential function ($y = ae^{bx}$).

set times were obtained from the best-fitted curve as the exponential function ($y = ae^{bx}$). It was shown that the setting time was dependent on the replacement ratio of GGBS; an increase in the GGBS content in the binder system resulted in an increase in the time for the initial and final sets, respectively, except for the case of CAC 80. For example, CAC 100 showed a rapid setting, of which the time to reach the initial and final sets was accounted for 185 and 230 min, respectively, while CAC 40 indicated 133 min and 204 min, respectively. It is notable that CAC 40 ranked the highest value for the setting time (188 and 240 min. for the initial and final sets, respectively). As the hydration process in the CAC is governed by the concentration of Ca^{2+} and $Al(OH)_4^-$ ions in solution, the amount of the hydraulic phases and its solubility could be influenced on the setting and hardening of the matrix at an early age [32, 34]. Moreover, the substitution of cement by supplementary cementitious materials, such as GGBS and PFA, would encourage the hydraulic reaction in the blends system, producing more space and water for hydration [32]. It was confirmed by isothermal calorimetry analysis in this study that the curve for total heat released for 24 hours, which was normalized to CAC content, showed the remarkably highest value, compared to the case of CAC 100. In fact, as the GGBS has a lower density than CAC, the increase of GGBS content in the CAC-GGBS system results in an increase in the average volume at the given mass, thereby providing more available space for hydration. Also, relative content of water for CAC particles (i.e., W/C ratio) increases with the higher content of GGBS in the binary system. Consequently, reactive grains (i.e., CA clinker) in the cement would be more probable for reacting with water to form CAC hydration products in the early hydration. However, there was a marginal influence of GGBS replacement on setting time for the case of CAC 80.

The compressive strength for CAC mortars with the different replacement ratios of GGBS was measured at 1–365 days, as shown in Figure 6. It was seen that the strength for CAC mortars partially substituted by GGBS performed a lower strength at the early ages but continuously increased at a given curing regime for all ages, showing no reduction in the strength. For example, the compressive strength for CAC-GGBS blends at 1 day was 31.6, 23.3, and 18.6 for CAC 80, 60, and 40, respectively. In particular, CAC 60 showed a remarkable high final strength, reaching beyond 57.5 MPa at 365 days, of which the value is superior to the strength for specimen made with CAC 100%, while CAC 80 and 40 were accounted for 49.4 and 43.8 MPa, respectively. In fact, CAC specimens usually produce the sudden loss of the strength in the hydration period depending on environmental conditions, presumably due to the conversion process, of which hexagonal phases of CAH_{10} and C_2AH_8 formed at normal temperatures would be imposed the transformation into cubic ones (C_3AH_6 and AH_3) [17–20]. This phenomenon was observed in this study that the strength for CAC 100 rapidly increased up to 7 days then faced a marginal decrease from 40.8 MPa at 7 days to 38.9 MPa at 28 days, which in turn reincreased with time (45.8 MPa at 365 days), presumably due to a further reaction of the remained grains with a released water from the conversion reaction. The CAC used in this study has calcium aluminates containing silicates (gehlenite; C_2AS), as the secondary phase, which could be reacted with water to form stratlingite (C_2ASH_8) in the long term. It was reported that an increase in curing temperature for the first 24 hours resulted in an increase in the hydration degree of C_2AS and the amount of C_2AH_8 hydrate at above 38°C [28]. In the previous studies [30–32], moreover, it was stated that addition of a siliceous binder to CAC produced a steady development of the strength over time,

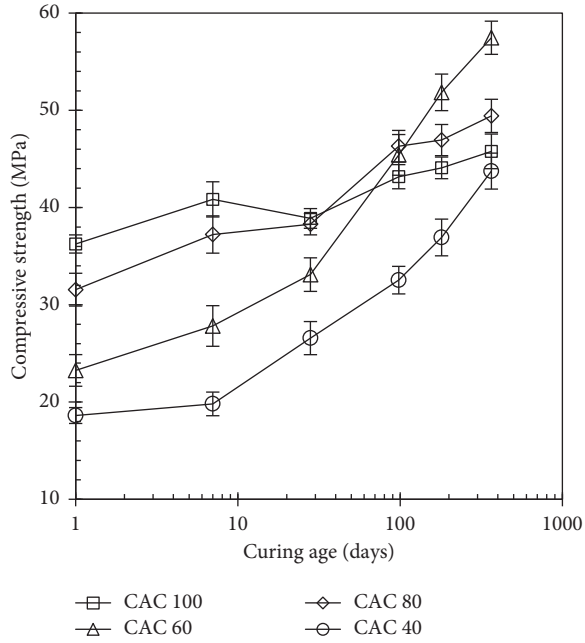

Figure 6: Compressive strength for mortar of CAC-GGBS mixtures with time. The error bars represent the standard deviation of measurements in six separate specimens for each mix ($n = 6$).

which is presumably due to the formation of C_2ASH_8. In particular, the initially formed C_2AH_8 hydrate would favor the reaction with silicates released from the binder [29]. However, CAC 40 possessed a marginal CA and C_2AS for hydration, thereby exhibiting a steadily increasing strength, but the lower values at all ages. It may imply that replacement content of GGBS in the CAC-GGBS system should be determined, considering the requirement for on site.

3.4. Modification of Pore Distribution. The pore distribution of mortar in the binary binder system of CAC and GGBS at 365 days was determined by MIP to investigate the influence of GGBS replacement on the pore structure in the CAC matrix, as given in Figure 7. The MIP curves were rendered by the incremental intrusion and their cumulative volume with different sizes. The total pore volume was affected by the GGBS content in CAC; an increase in the replacement ratio of GGBS resulted in a decrease in the total intruded content of mercury into the specimen, except for CAC 40, of which the value was accounted for 0.145, 0.140, and 0.131 mL/g for CAC 100, 80, and 70, respectively. As seen in Figure 4, CAC 100 showed the overall transformation of C_2AH_8 phase into C_3AH_6 and AH_3 ones over time. It may be attributed to a higher density of cubic phases, increasing the distance between the hydrates and thus the porous matrix in the mortar. Moreover, an increased porosity of the matrix may decrease the development of the strength during hydration periods. In fact, CAC 100 showed the sudden decrease in the strength at 28 days, as seen in Figure 6, which in turn reincreased up to 365 days of curing presumably due to a further reaction with a surplus of water from the conversion reaction. In the presence of GGBS in mixture, in contrast, the conversion reaction (equation (2)) was prevented by the transformation of the C_2AH_8 phase into C_2ASH_8 through the hydration duration, of which the stable hydrate is similar to unstable hydrate in density (1.937 and 1.950 for C_2ASH_8 and C_2AH_8, respectively) [35, 36]. This change of composition in the matrix would produce the densified pore structure and thus a decrease in the porosity at the total. Despite modification of the matrix in the CAC-GGBS mixture, the higher ratio of GGBS replacement imposed an increased total intrusion volume (0.149 mL/g) presumably due to deficiency of hydraulic phases, as already mentioned. However, there was no particular relation in the intrusion volume at a given realm, which was in the range below 0.05 and 0.05–10 and above 10 μm for small capillaries, large capillaries, and voids, respectively.

3.5. Variation of Stoichiometric Composition. The surfaces of the fragment for cement paste of CAC-GGBS mixtures cured at 365 days were investigated using SEM analysis, as shown in Figure 8. A presence of strätlingite was obviously detected at all samples, of which the hydrates had the morphology of hexagonal plates, sometimes a thin flaky plate, and in addition, the phase seemed to be more accommodated in the matrix at pastes substituted by GGBS. To compare atomic ratios (Ca/Al and Si/Al) at the C_2ASH phase in the paste of the binary mixtures, EDS analysis was simultaneously performed, measuring the 30 spots for each sample. It was clearly shown that an increase of GGBS content in the mixture resulted in an increase in the ratio of Si/Al and a decrease in Ca/Al ratio, of which an ideal ratio in the C_2ASH_8 phase is 0.5 and 1.0 for Si/Al and Ca/Al, respectively. It may be attributed to the increased GGBS content, from which the large amounts of silicate ions would

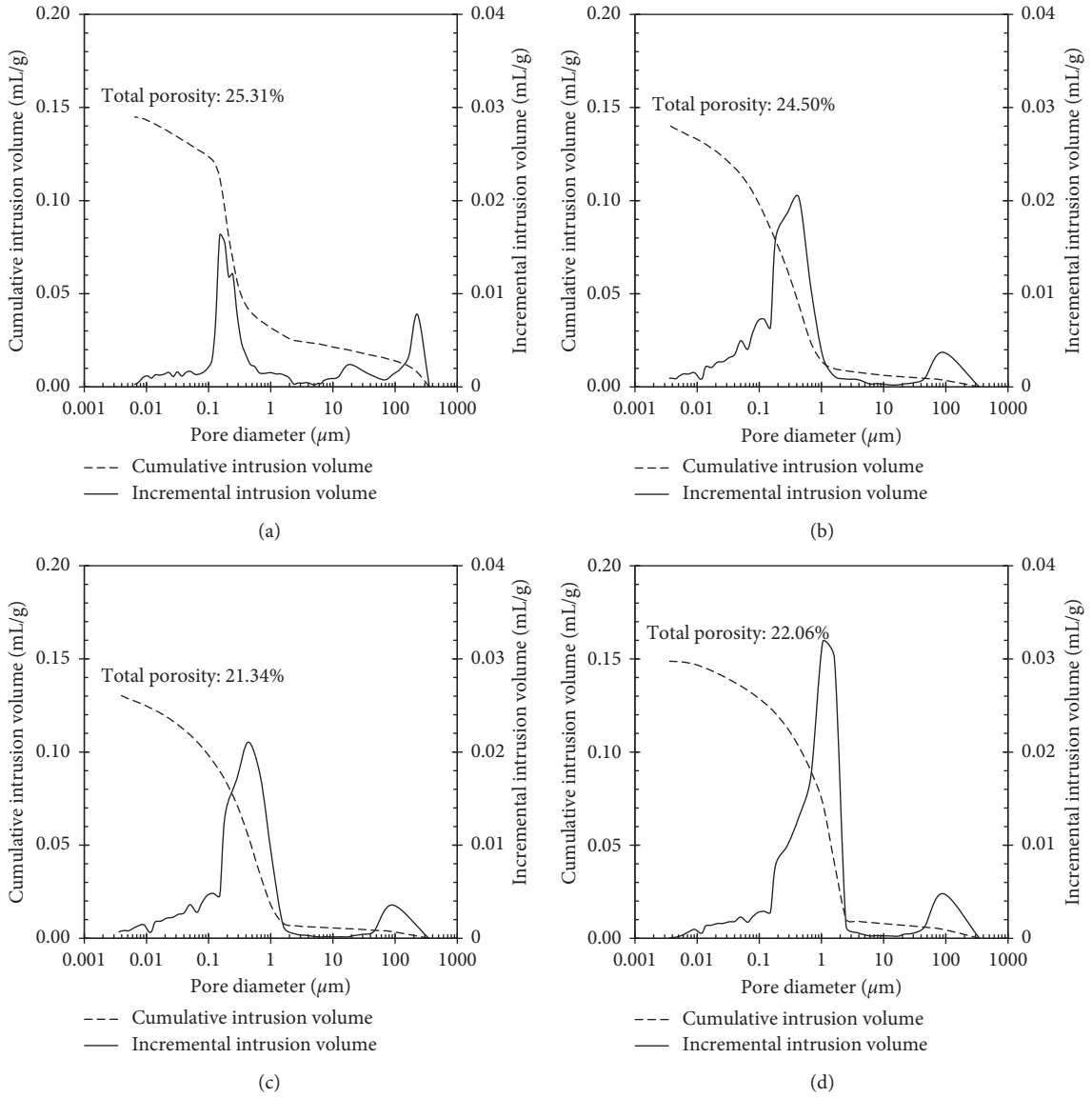

Figure 7: MIP results, rendered by incremental and cumulative intrusion volume with pore diameter, for mortar of CAC-GGBS mixtures: (a) CAC 100; (b) CAC 80; (c) CAC 60; (d) CAC 40.

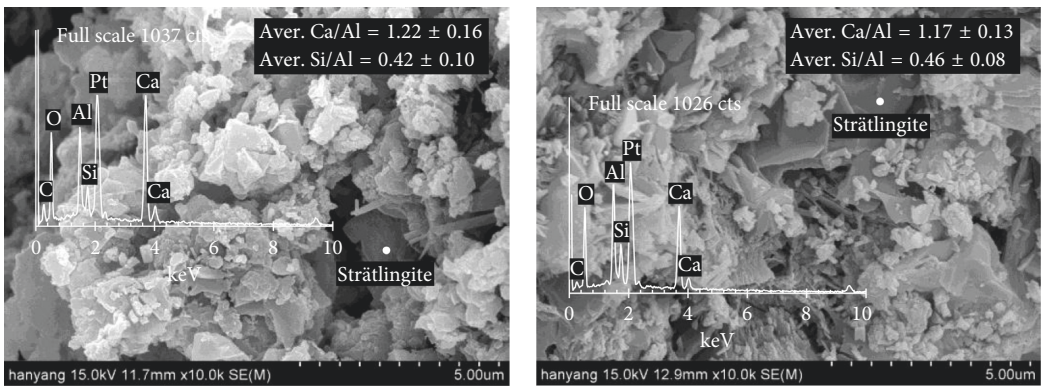

Figure 8: Continued.

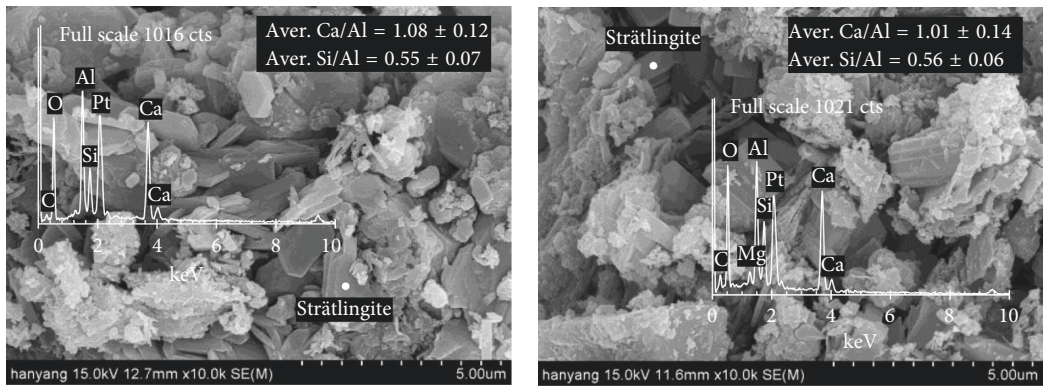

(c) (d)

Figure 8: Microscopic observation for the formation of strätlingite in paste of CAC-GGBS mixtures at 365 days of curing. The standard deviation is derived from the measurements in 30 spots for each sample ($n = 30$): (a) CAC 100; (b) CAC 80; (c) CAC 60; (d) CAC 40.

be released into the pore solution during long-term hydration. As already mentioned in Section 3.3, the formation of strätlingite is affected by the amounts of dissolved silica from the siliceous materials. In addition, the stoichiometric structure is dependent on the surrounding chemical composition supplied from the grains in the solution [10, 37]. As a higher content of pozzolanic materials in a mixture produces more silicates into the solution, a probable to form silica-rich strätlingite would be increased. Thus, CAC 40 produced the highest ratio of Si/Al in the C_2ASH_8 phase, while the lower Si/Al ratio (0.42 ± 0.10) was observed at the paste made with CAC solely. However, there was no further experimentation supporting the differences of atomic ratios between CAC-GGBS mixture.

4. Conclusions

In this study, an influence of additive material containing silica on fundamental properties of CAC was investigated by development of strength, which was supported by further experimental work including hydration behavior at initial and long-term duration using isothermal calorimetry and X-ray diffraction analysis and an examination of the pores structure from mercury intrusion porosimetry. Microscopic observation for the morphology of strätlingite was performed by scanning electron microscopy, together with energy dispersive spectroscopy. The GGBS was replaced as binder with 0, 20, 40, and 60% by weight of the mass. Details derived from the present study are given as follows:

(1) An increase in the GGBS content in the mixture, kept at 0.4 of W/B, resulted in an increase in the rate of heat evolved within 0–2 hours, in addition to the total heat released for 24 hours, in isothermal calorimetry normalized to CAC content. This may be supposed to available space in the matrix at early ages, arising from a lower density of the binary system with the increase of GGBS content.

(2) Setting time, in terms of initial and final sets, was decreased with the increase of GGBS content, due to large amounts of water and space for hydration at the early ages, except for the case of CAC 80. All CAC-GGBS mixed mortars exhibited a gradual development of strength with time, ranging from 43.8–57.5 MPa at 365 days, while the specimen made with CAC solely gained the strength rapidly at the early ages (40.8 MPa at 7 days), which subsequently faced to a sudden reduction due to conversion and then reincreased up to 45.8 MPa at 365 days.

(3) The continuous increase in the strength for mixtures of CAC-GGBS was supported by XRD curves, showing a decrease in the peak intensity for the C_2AH_8 phase and simultaneously an increase in that for stratlingite with time. It may imply that the presence of GGBS prevents the conversion reaction to stable hydrates from metastable ones. However, C_2AH_8 in CAC 100 was fully transformed into C_3AH_6 and AH_3 after 28 days of curing at a given curing regime.

(4) A modification of the pore structure, in terms of total porosity, was clearly shown that the increase of GGBS replacement ratio resulted in a decrease in the total intrusion volume of mercury at 365 days, except for the case of CAC 40, which may be attributed to a marginal CAC particle in the long-term hydration.

(5) The formation of strätlingite in the paste cured at 365 days was confirmed by microscopic observation using SEM at all CAC-GGBS mixtures. The stoichiometric composition of the phase was in the range of 0.42–0.56 and 1.01–1.22 for atomic ratio of Si/Al and Ca/Al, irrespective of GGBS content in the mixtures.

Data Availability

The data used to support the findings of this study are included within the article.

Conflicts of Interest

The authors declare that they have no conflicts of interest.

Acknowledgments

This research was supported by a grant (18CTAP-C132998-02) from Technology Advancement Research Program funded by Ministry of Land, Infrastructure and Transport of Korean government.

References

[1] The Concrete Society, *Calcium Aluminate Cements in Construction—A Re Assessment*, Concrete Society Technical Report 46, The Concrete Society, Camberley, UK, 1997.

[2] K. L. Scrivener, "100 years of calcium aluminate cements," in *Proceedings of International Conference on Calcium Aluminate Cements*, pp. 3–6, Avignon, France, June 2008.

[3] A. Neville, "History of high-alumina cement. Part I: problems and the stone report," *Engineering History and Heritage*, vol. 162, no. 2, pp. 81–91, 2008.

[4] F. A. Cardoso, M. D. M. Innocentini, M. M. Akiyoshi, and V. C. Pandolfelli, "Effect of curing time on the properties of CAC bonded refractory castables," *Journal of the European Ceramic Society*, vol. 24, no. 7, pp. 2073–2078, 2004.

[5] C. Parr, D. Verat, C. Wöhrmeyer et al., "High purity calcium aluminate binders for demanding high temperature applications," in *Proceedings of International Conference on Calcium Aluminate Cements*, pp. 417–428, Avignon, France, June 2008.

[6] A. Buhr, D. Schmidtmeier, G. Wams et al., "Testing of calcium aluminate cement bonded castables and influence of curing conditions on the strength development," in *Proceedings of International Conference Calcium Aluminate Cements*, pp. 437–449, Avignon, France, June 2008.

[7] K. L. Scrivener, J.-L. Cabiron, and R. Letourneux, "High-performance concretes from calcium aluminate cements," *Cement and Concrete Research*, vol. 29, no. 8, pp. 1215–1223, 1999.

[8] M. G. Alexander and C. Fourie, "Performance of sewer pipe concrete mixtures with portland and calcium aluminate cements subject to mineral and biogenic acid attack," *Materials and Structures*, vol. 44, no. 1, pp. 313–330, 2010.

[9] J. Herisson, E. D. V. Hullebusch, M. Guéguen-Minerbe et al., "Biogenic Corrosion Mechanism: Study of Parameters Explaining Calcium Aluminate Cement Durability," in *Proceedings of International Conference on Calcium Aluminate Cements*, pp. 633–644, Avignon, France, May 2014.

[10] K. L. Scrivener and A. Capmas, "13. Calcium aluminate cements," in *Lea's Chemistry of Cement and Concrete*, pp. 713–782, Elsevier Science & Technology, Amsterdam, Netherlands, 2003.

[11] R. D. Lute, "Durability of calcium-aluminate based binders for rapid repair application," Doctoral thesis, The University of Texas at Austin, Austin, TX, USA, 2016.

[12] Texas Department of Transportation, *Special Specification 4491: Type CAC Concrete*, Texas Department of Transportation, Austin, TX, USA, 2009.

[13] H. G. Midgley and A. Midgley, "The conversion of high alumina cement," *Magazine of Concrete Research*, vol. 27, no. 91, pp. 59–77, 1975.

[14] C. Bradbury, P. M. Callaway, and D. D. Double, "The conversion of high alumina cement/concrete," *Materials Science and Engineering*, vol. 23, no. 1, pp. 43–53, 1976.

[15] S. Rashid and X. Turrillas, "Hydration kinetics of $CaAl_2O_4$ using synchrotron energy-dispersive diffraction," *Thermochimica Acta*, vol. 302, no. 1-2, pp. 25–34, 1997.

[16] T. R. Jensen, A. N. Christensen, and J. C. Hanson, "Hydrothermal transformation of the calcium aluminum oxide hydrates $CaAl_2O_4{\cdot}10H_2O$ and $Ca_2Al_2O_5{\cdot}8H_2O$ to $Ca_3Al_2(OH)_{12}$ investigated by in situ synchrotron X-ray powder diffraction," *Cement and Concrete Research*, vol. 35, no. 12, pp. 2300–2309, 2005.

[17] D. C. Teychenné, "Long-term research into the characteristics of high alumina cement concrete," *Magazine of Concrete Research*, vol. 27, no. 91, pp. 78–102, 1975.

[18] R. J. Collins and W. Gutt, "Research on long-term properties of high alumina cement concrete," *Magazine of Concrete Research*, vol. 40, no. 145, pp. 195–208, 1988.

[19] K. Y. Ann, T.-S. Kim, J. H. Kim, and S.-H. Kim, "The resistance of high alumina cement against corrosion of steel in concrete," *Construction and Building Materials*, vol. 24, no. 8, pp. 1502–1510, 2010.

[20] M. P. Adams and J. H. Ideker, "Influence of aggregate type on conversion and strength in calcium aluminate cement concrete," *Cement and Concrete Research*, vol. 100, pp. 284–296, 2017.

[21] G. Falzone, M. Balonis, and G. Sant, "X-AFm stabilization as a mechanism of bypassing conversion phenomena in calcium aluminate cements," *Cement and Concrete Research*, vol. 72, pp. 54–68, 2015.

[22] H. G. Midgley and P. B. Rao, "Formation of stratlingite, $2CaO.SiO_2.Al_2O_3.8H_2O$, in relation to the hydration of high alumina cement," *Cement and Concrete Research*, vol. 8, no. 2, pp. 169–172, 1978.

[23] A. J. Majumdar, R. N. Edmonds, and B. Singh, "Hydration of secar 71 aluminous cement in presence of granulated blast furnace slag," *Cement and Concrete Research*, vol. 20, no. 1, pp. 7–14, 1990.

[24] A. J. Majumdar, B. Singh, and R. N. Edmonds, "Hydration of mixtures of 'Ciment Fondu' aluminous cement and granulated blast furnace slag," *Cement and Concrete Research*, vol. 20, no. 2, pp. 197–208, 1990.

[25] A. J. Majumdar and B. Singh, "Properties of some blended high-alumina cements," *Cement and Concrete Research*, vol. 22, no. 6, pp. 1101–1114, 1992.

[26] M. Collepardi, S. Monosi, and P. Piccioli, "The influence of pozzolanic materials on the mechanical stability of aluminous cement," *Cement and Concrete Research*, vol. 25, no. 5, pp. 961–968, 1995.

[27] J. Ding, Y. Fu, and J. J. Beaudoin, "Strätlingite formation in high alumina cement - silica fume systems: significance of sodium ions," *Cement and Concrete Research*, vol. 25, no. 6, pp. 1311–1319, 1995.

[28] C. Gosselin, E. Gallucci, and K. Scrivener, "Influence of self heating and Li2SO4 addition on the microstructural development of calcium aluminate cement," *Cement and Concrete Research*, vol. 40, no. 10, pp. 1555–1570, 2010.

[29] B. Pacewska, M. Nowacka, and M. Aleknevičius, "Investigation of early hydration of high aluminate cement-based binder at different ambient temperatures," *Journal of Thermal Analysis and Calorimetry*, vol. 109, no. 2, pp. 717–726, 2012.

[30] N. Y. Mostafa, Z. I. Zaki, and O. H. Abd Elkader, "Chemical activation of calcium aluminate cement composites cured at elevated temperature," *Cement and Concrete Composites*, vol. 34, no. 10, pp. 1187–1193, 2012.

[31] Ö. Kirca, Ö. Yaman, and M. Tokyay, "Compressive strength development of calcium aluminate cement-GGBFS blends," *Cement and Concrete Composites*, vol. 35, no. 1, pp. 163–170, 2013.

[32] C. Gosselin, "Microstructural development of calcium aluminate cement based systems with and without supplementary cementitious materials," Doctoral thesis, Swiss Federal Institute of Technology in Lausanne, Lausanne, Switzerland, 2009.

[33] ASTM International, *ASTM C403/C403M-16 Standard Test Method for Time of Setting of Concrete Mixtures by Penetration Resistance*, ASTM International, West Conshohocken, PA, USA, 2016.

[34] J. H. Ideker, "Early-age behavior of calcium aluminate cement systems," Doctoral thesis, The University of Texas at Austin, Austin, TX, USA, 2008.

[35] H. Fryda, E. Charpentier, and J. M. Bertino, "Accelerated test for conversion of calcium aluminate cement concrete," in *Proceedings of International Conference on Calcium Aluminate Cements*, pp. 159–169, Avignon, France, June 2008.

[36] M. Balonis and F. P. Glasser, "The density of cement phases," *Cement and Concrete Research*, vol. 39, no. 9, pp. 733–739, 2009.

[37] D. L. Rayment and A. J. Majumdar, "Microanalysis of high-alumina cement clinker and hydrated HAC/slag mixtures," *Cement and Concrete Research*, vol. 24, no. 2, pp. 335–342, 1994.